# First passage time statistics of non-Markovian random walker: Dynamical response approach

Yuta Sakamoto and Takahiro Sakaue [*]

*Department of Physical Sciences, Aoyama Gakuin University, 5-10-1 Fuchinobe, Chuo-ku, Sagamihara, Japan*

A non-Markovian process, in which stochastic evolution of the system depends on its past history, often shows up in soft matter, living cells, and other complex systems. Despite its importance, however, the statistics of first passage time in such systems is not well understood. This is largely due to the fact that most theoretical frameworks are based on Markovian description, and incorporation of the memory effect into the problem remains a challenge. Here, we argue that a key quantity in the problem, i.e., the average behavior of a non-Markovian walker after the first passage, can be linked to its dynamical response, and propose a simple framework to compute important observables in the first passage problem. We perform a mean-field analysis and demonstrate semiquantitative description of the one-dimensional fractional Brownian motion in the presence of an absorbing boundary.

## I. INTRODUCTION

How long does it take for a random walker to reach a destination? Such a question on the first passage time (FPT) is relevant to a broad range of situations in science, technology, and everyday life applications as encountered, for instance, in diffusion-limited reactions [1–3], barrier crossing [4–7], target search processes [8,9], cyclization of DNA molecules [10–13], price fluctuation in the market [2], and spread of diseases [14]. Today, the concept of the FPT and its importance in the study of stochastic processes are well recognized, and theoretical methods for its computation are standardized [1,2]. However, most of them are devised for Markovian random walkers, whose decision-making does not depend on its past history, and thus are not applicable to non-Markovian walkers despite their ubiquitousness.

Indeed, a growing body of evidence suggests that the non-Markovian dynamics is found quite generally in rheologically complex matters typically, but not exclusively, with viscoelastic properties. Classical examples are found in the diffusion of interacting particles in narrow channels [15] and the motion of tagged monomers in long polymer chains [16,17]. Other notable representatives include colloidal particles in polymer solutions [18] or nematic solvents [19], lipids molecules and cholesterols in cellular membrane [20], proteins in crowded media [21], and chromosome loci [22] as well as membrane-less organelles in living cells [23].

Such systems commonly exhibit a slow dynamics in the form of subdiffusion $\text{MSD}(t) \sim t^{\alpha}$ characterized by the anomalous exponent $\alpha < 1$, where $\text{MSD}(t)$ stands for the mean-square displacement of the observed particle during the time scale $t$. Here, the physical mechanism at work is the interaction of the observed degree of freedom with the collective modes with a broad range of time scales underlying the complex environment. Because of its importance in, e.g., intracellular transport, the theoretical tools to describe and diagnose such anomalous diffusion phenomenology have been well developed in the last few decades [24]. However, most of them rely on MSD and related quantities, while much less attention has been paid to the FPT, despite its fundamental and practical importance to characterize the underlying stochastic process. This is particularly true for systems possessing *memory*, as nontrivial information on the history dependence of the system is encoded in the FPT statistics [25]. It has long been known that the anomalous transport properties affect the rates of chemical and biochemical reactions [26], and such reactions are initiated by the encounter of reactant molecules, so precisely quantified by means of the FPT statistics.

Unfortunately, our current understanding on the FPT of non-Markovian walker lags far behind that of its Markovian counterpart, where the difficulty is largely associated with the lack of an appropriate theoretical foothold [25,27,28]. While the Fokker-Planck equation and its related methods play a key role in analyzing the time evolution of the probability distribution of the Markovian walkers, their careless application is problematic for walkers with memory, a defining property of the non-Markovian process. At present, available results are quite limited, with notable examples being the perturbative and scaling arguments to estimate the asymptotic exponents characterizing the distribution of FPT and related quantities in the unbounded domain [25,29–31], some approximation schemes to calculate the mean FPT of the polymer looping process [3,10–13], and more recent analytical treatment to compute the mean FPT in confined domains [28]. However, neither the full distribution of FPT or the position distribution of non-Markovian walkers in the presence of the boundary

---

[*]Corresponding author: sakaue@phys.aoyama.ac.jp
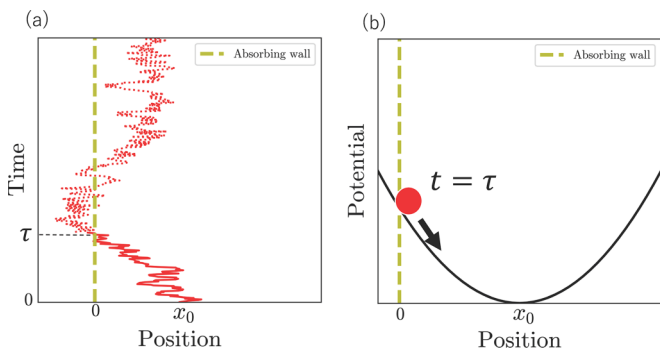
FIG. 1. (a) Example trajectory of fBM with $\alpha = 0.5$ starting from the initial position $x = x_0$. Before (after) the first hitting on the absorbing boundary at $x = 0$, the trajectory is drawn by a solid (dotted) curve. The first passage event can be viewed as a large fluctuation to create a nonequilibrium state at $t = \tau$. (b) The average behavior after the first passage ($t > \tau$) resembles the relaxation process; for subdiffusive fBM, the viscoelastic memory effect is represented by the harmonic restoring force, whose spring constant gets smaller algebraically in longer time scales [17].

are available, making the computation of these quantities in non-Markovian processes a fundamental challenge.

One way to analyze the FPT statistics is to look at the behaviors of random walkers *after* the first passage (Fig. 1). Along this line, a basic starting point is a renewal equation, which has proved to be useful, at least, to the Markovian case [2]. Our aim here is to find a way to incorporate the memory effect into the renewal-type framework. To this end, we argue that the essential aspect of the memory effect is encoded in the dynamical response of the system, which could thus be linked to the walker's average behavior after the first passage. Although nontrivial, this link allows us to construct a simple mean-field framework to calculate the FPT statistics of non-Markovian walkers, to verify earlier scaling formulas, and to propose the approximate functional form of the FPT distribution over entire time scales, and also the walker's position probability distribution function. Importantly, our formalism allows one to unveil how and why the textbook standard "method of image" [2,32] breaks down by pinpointing the role of memory built up during the first passage process. Here, we focus on the subdiffusive fractional Brownian motion [33] (fBM with $\alpha < 1$), an important class of non-Markovian walkers found in widespread complex systems including living cells and nuclei [20–23].

## II. FRAMEWORK

### A. Random walker with power-law memory

As a paradigm, consider a random walker in one-dimensional half space with an absorbing boundary at the origin. A walker is initially positioned at $x = x_0(> 0)$ at $t = 0$, and evolves according to the equation $\dot{x}(t) = \eta(t)$, where $\dot{x} = dx(t)/dt$ and $\eta(t)$ is the fractional Gaussian noise, which is characterized by its stationarity and long-lasting temporal correlation. Specifically, for a large time scale, its autocorrelation decays according to the power law $\langle \eta(t)\eta(t') \rangle \simeq -D_\alpha |t - t'|^{\alpha-2}$ ($0 < \alpha < 1$), with $D_\alpha$ being the generalized

diffusivity. For a walker in free space (no boundary), its position probability distribution $P(x, t; x_0)$ is simply given by $\mathcal{N}(x, x_0, 2D_\alpha t^\alpha)$, where $\mathcal{N}(x, A, B) = (2\pi B)^{-1/2} e^{(x-A)^2/2B}$ denotes Gaussian distribution of $x$ with the average $A$ and the variance $B$.

### B. Process after first passage

We now set a stage by introducing an absorbing boundary at the origin $x = 0$ such that the walker performs fBM in half space $x > 0$ with the same initial condition as before. Using the free space distribution $P(x, t; x_0)$, the walker's position probability $P_+(x, t; x_0)$ is now represented as

$$P_+(x, t; x_0) = P(x, t; x_0) - Q(x, t; x_0), \quad (1)$$

where $Q(x, t; x_0)$ is the position distribution of the *dead walker*, who touched the absorbing boundary by this moment. Note that while one usually looks at the walker's behavior in the physical domain ($x \geqslant 0$) up to the absorption ($t \leqslant \tau$) in the context of FPT, Eq. (1) holds in entire space and time domains in a spirit similar to Ref. [28]; the absorbing boundary at $x = 0$ necessitates $P(x, t; x_0) = Q(x, t; x_0)$ for $x \leqslant 0$.

Using the FPT distribution $F(\tau; x_0)$, $Q(x, t; x_0)$ is represented as

$$Q(x, t; x_0) = \int_0^t F(\tau; x_0) P(x, t; x_0 | \text{FPT} = \tau) d\tau, \quad (2)$$

where $P(x, t; x_0 | \text{FPT} = \tau)$ is the conditional probability of the walker's position at time $t$ after its first passage at time $\tau$. For the Gaussian process (including fBM), one expects the form

$$P(x, t; x_0 | \text{FPT} = \tau) = \mathcal{N}(x, \langle x(t) \rangle_{\text{FPT}=\tau}, \langle [\delta x(t)]^2 \rangle_{\text{FPT}=\tau}), \quad (3)$$

for $t > \tau$ with the mean $\langle x(t) \rangle_{\text{FPT}=\tau}$ and variance $\langle [\delta x(t)]^2 \rangle_{\text{FPT}=\tau}$ of the walker's position after the first passage at $t = \tau$.

Using Eq. (3) in Eq. (2), we integrate Eq. (1) over a half space ($x \geqslant 0$) to find the integral equation

$$1 - \text{erf}\left(\frac{x_0}{\sqrt{4D_\alpha t^\alpha}}\right) = \int_0^t F(\tau; 1)\{1 - \text{erf}[h(t, \tau)]\} d\tau, \quad (4)$$

with

$$h(t, \tau) \equiv \frac{\langle x(t) \rangle_{\text{FPT}=\tau}}{\sqrt{2\langle [\delta x(t)]^2 \rangle_{\text{FPT}=\tau}}}. \quad (5)$$

We note that Eq. (4) is exact aside from the Gaussianity assumption. In the absence of memory effect, $h(t, \tau) = 0$ as $\langle x(t) \rangle_{\text{FPT}=\tau} = 0$ irrespective of the starting position $x_0$. In this case, Eq. (4) immediately leads to the classical result of the survival probability $S(t; x_0) = 1 - \int_0^t F(t'; x_0) dt' = \text{erf}(x_0/\sqrt{4D_1 t})$ for the Markovian case [2], see also Sec. III D. Thus, all the non-Markovian effect is encoded in $h(t, \tau)$, which we call the memory function.

### C. Memory function and dynamical response

The memory function includes $\langle x(t) \rangle_{\text{FPT}=\tau}$ and $\langle [\delta x(t)]^2 \rangle_{\text{FPT}=\tau}$ as its ingredients. For the latter, we assume

$$\langle [\delta x(t)]^2 \rangle_{\text{FPT}=\tau} = 2D_\alpha (t - \tau)^\alpha, \quad (6)$$

which is motivated as a straightforward generalization of the Markovian result $\langle [\delta x(t)]^2 \rangle_{\text{FPT}=\tau} = 2D_1(t - \tau)$, and we have
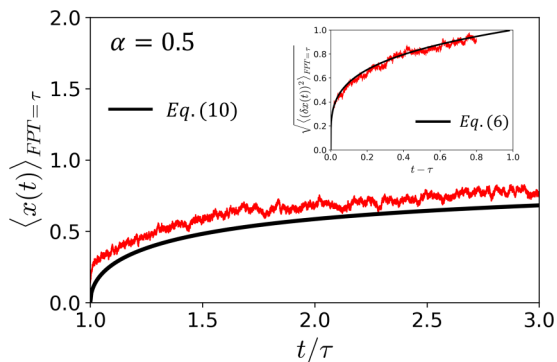
FIG. 2. Time evolution of the average $\langle x(t) \rangle_{\text{FPT}=\tau}$ and (inset) variance $\langle [\delta x(t)]2 \rangle_{\text{FPT}=\tau}$ of the position of fBM ($\alpha = 0.5$) after the first passage at $t = \tau$. Units of length and time are $x_0$ and $\tau_{x_0}$, respectively (see the text). Shown is the numerical data from the subensemble with $\tau = 0.2$ compared to the formulas (thick black curves) Eqs. (10) and (6).

indeed checked that Eq. (6) agrees well with the numerical simulation result (Fig. 2 inset), see also Fig. 8 in Appendix B. On the other hand, the Markovian result $\langle x(t) \rangle_{\text{FPT}=\tau} = 0$ for the former does not provide any clue for its non-Markovian generalization. A rigorous calculation of $\langle x(t) \rangle_{\text{FPT}=\tau}$ for the general non-Markovian process would be a formidable task. Below we seek an alternative quantity, which also captures the memory effect of the non-Markovian walker, and can be compared to $\langle x(t) \rangle_{\text{FPT}=\tau}$ through the analysis of dynamical response of the system.

To this end, we generalize the time evolution equation of fBM by including the time-dependent external force $f(t)$ [17],

$$\dot{x}(t) = \int_{-\infty}^{t} \mu(t - t') f(t') dt' + \eta(t), \qquad (7)$$

where $\mu(t)$ is the mobility kernel, which is related to the noise autocorrelation via the fluctuation-dissipation relation $\langle \eta(t) \eta(t') \rangle = T \mu(|t - t'|)$ with $T$ being the noise strength. Now consider that we switch on the force at $t = 0$, operate it according to some protocol $f(t)$, and switch off at $t = \tau$. Using Eq. (7), one can calculate the average position of the walker $\langle x(t) \rangle_f$, where the subscript ($f$) indicates the external forcing over $0 < t \leqslant \tau$. For the Markovian case, the average position evolves until $t = \tau$ and stays at $\langle x(\tau) \rangle_f$ after turning the force off ($t > \tau$) because of its memory-less nature. However, the relaxation process follows for the non-Markovian case due to the memory effect; for fBM, it can be viewed as the relaxation in harmonic potential field, whose spring constant decays algebraically with the time scale. To link such a memory effect in dynamical response to the FPT problem, we require the condition $\langle x(\tau) \rangle_f = 0$, see Fig. 1. This corresponds to a necessary condition for the first passage at $t = \tau$, making the otherwise unrelated two quantities $\langle x(t) \rangle_{\text{FPT}=\tau}$ and $\langle x(t) \rangle_f$ apposable. Our conjecture is stated as follows: there exists a specific force protocol $f(t)$ such that $\langle x(t) \rangle_{\text{FPT}=\tau} = \langle x(t) \rangle_f$ for $t > \tau$.

### D. Mean-field approximation

A proof of the conjecture would be as difficult as solving the original FPT problem. Here, we employ the simplest

scenario of the constant force (dubbed temporal "mean-field") protocol and examine its predictability through quantitative comparison with numerical simulation. With yet undetermined force magnitude $f_0$, the protocol is now $f(t) = f_0$ for $0 < t \leqslant \tau$ and $f(t) = 0$ for $t > \tau$. From Eq. (7), we obtain

$$\langle \dot{x}(t) \rangle_f = f_0 \times \begin{cases} \int_0^t \mu(t - t') dt' & (t \leqslant \tau) \\ \int_0^\tau \mu(t - t') dt' & (t > \tau). \end{cases} \qquad (8)$$

The "self-consistent" FPT condition $\langle x(\tau) \rangle_f = 0$ determines the force magnitude

$$f_0 = -\frac{T x_0}{D_\alpha} \tau^{-\alpha}. \qquad (9)$$

As already stated, for the Markovian case $\mu(t - t') \sim \delta(t - t')$, Eq. (8) (second line) results in $\langle \dot{x}(t) \rangle_f = 0$, thus $\langle x(\tau) \rangle_f = 0$ for $t > \tau$. For the non-Markovian case, however, the time integral of Eq. (8) (second line) with Eq. (9) leads to a nontrivial relaxation behavior (see Appendix A),

$$\langle x(t) \rangle_f = x_0 \left[ 1 + \left( \frac{t - \tau}{\tau} \right)^\alpha - \left( \frac{t}{\tau} \right)^\alpha \right] \quad (t > \tau). \qquad (10)$$

Combined with our conjecture, we obtain the memory function

$$h(t, \tau) = \frac{1}{\sqrt{2(t - \tau)^\alpha}} \left[ 1 + \left( \frac{t}{\tau} - 1 \right)^\alpha - \left( \frac{t}{\tau} \right)^\alpha \right]. \qquad (11)$$

Note that, from here onwards, we measure the length and the time in units of $x_0$ and $\tau_{x_0} = (x_0^2 / 2 D_\alpha)^{1/\alpha}$, respectively, which are the sole characteristic length and time scales in the problem, making the initial position $x_0 = 1$ upon rescaling.

Before proceeding to the analysis of integral equation (4), let us check how Eq. (10) works as a proxy for $\langle x(t) \rangle_{\text{FPT}=\tau}$. Comparison with numerical simulation (Fig. 2 for $\alpha = 0.5$ and $\tau = 0.2$) shows a reasonable agreement between Eq. (10) and $\langle x(t) \rangle_{\text{FPT}=\tau}$. However, we note that the average relaxation behavior of fBM after the first passage is far more involved than our mean-field result indicates; see Appendix B for detailed analysis, which reveals a systematic deviation from Eq. (10) more evidently for smaller $\alpha$. Nevertheless, we show below that our framework with the memory function (11) provides a reasonably good description for several key quantities in FPT statistics, and also yields the correct nontrivial scaling exponents characterizing the asymptotic behaviors of fBM in the presence of an absorbing boundary [25,29–31].

### III. RESULTS AND DISCUSSION

#### A. First passage time distribution

We now determine the leading order solution of Eq. (4) in the form

$$F(\tau; 1) = \mathcal{C}_\alpha \exp \left[ -\frac{1}{2\tau^\omega} \right] \tau^{-(1+p)}, \qquad (12)$$

where $\mathcal{C}_\alpha$ is a normalization constant. This function, a generalization of the Markovian result [2] $\omega = 1$, $p = 1/2$, exhibits a peak at $\tau = \tau^* = [\omega / 2(1 + p)]^{1/\omega}$, and develops a power-law tail $F(\tau; 1) \sim \tau^{-(1+p)}$ at $\tau \gg \tau^*$. With this in mind, we plug the ansatz (12) into Eq. (4) and perform the asymptotic analysis in the long time limit ($t \gg 1$), which yields $p = 1 - \alpha/2$
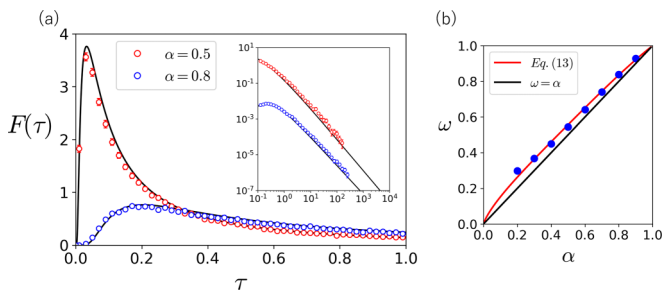
FIG. 3. (a) FPT distribution $F(\tau; 1)$ for subdiffusive fBM ($\alpha = 0.8, 0.5$). Inset shows the double logarithmic plot of the large $\tau$ regime, where the asymptotic slope $p + 1 = 2 - \alpha/2$ is clearly visible. The data for $\alpha = 0.8$ is shifted downward ($\times 10^{-2}$) for visual clarity. Both in the main panel and the inset, symbols represent simulation results and the curves correspond to the analytical formula (12), with $p = 1 - \alpha/2$ and $\omega$ given by Eq. (13). The error bars represent 95% CI. (b) Exponent $\omega$ as a function of $\alpha$, which characterizes the early time regime in FPT distribution. Blue solid circles are obtained by fitting the numerical simulation data for several $\alpha$ values [two of them shown in Fig. 3(a)] with the formula (12). Fitting these data with Eq. (13) fixes the parameter $c_1 = 0.12$.

in agreement with the previous scaling argument [25,29] (see Appendix C). In addition, our formulation allows us to obtain the exponent $\omega$, which satisfies the relation

$$\frac{(2-\alpha)^{2\omega}(2+\alpha)^{\alpha}}{\omega^{\alpha}} = 3^{\omega}c_1^{\omega(\alpha-1)} \tag{13}$$

with a numerical constant $c_1$ of order unity (see Appendix C).

In Fig. 3, we compare our analytical formula for $F(\tau; 1)$ with the results obtained from numerical simulation. As shown, the agreement is excellent, encompassing the short time singularity to the peak and the eventual long time power-law tail, which are characterized by the exponents $\omega$ and $p$, respectively. The peak position $\tau^*$ is rather sensitive to the value of $\omega$. This is particularly true for small $\omega$, which is the case for the small $\alpha$, shifting the peak position $\tau^*$ vanishingly small in the limit $\alpha \to 0$.

### B. Probability distributions of dead walkers

We are now in a position to take a close look at $Q(x, t; 1)$, which is the distribution of walkers after their first passage. From Eqs. (2) and (3), we immediately find that the memory effect in the form of restoring force represented by nonzero $\langle x(t) \rangle_{\mathrm{FPT}=\tau}$ (Fig. 2) breaks the reversal symmetry with respect to $x = 0$, i.e., $Q(x, t; 1) \neq Q(-x, t; 1)$ that clearly manifests the breakdown of the image method, see Sec. III D below for further discussion.

### C. Probability distributions of survived walkers

Given the analytical predictability of $Q(x, t; 1)$ shown in Fig. 4, we proceed to plot in Fig. 5 the normalized position probability $\tilde{P}_+(x, t; 1) \equiv P_+(x, t; 1)/S(t; 1)$ of the survival walker from Eq. (1). Again, our prediction captures all the salient features seen in numerical simulations, but one starts to see a deviation for small $\alpha$ in the long time regime, which is ascribed to the error in representing $\langle x(t) \rangle_{\mathrm{FPT}=\tau}$ through our mean-field estimate.
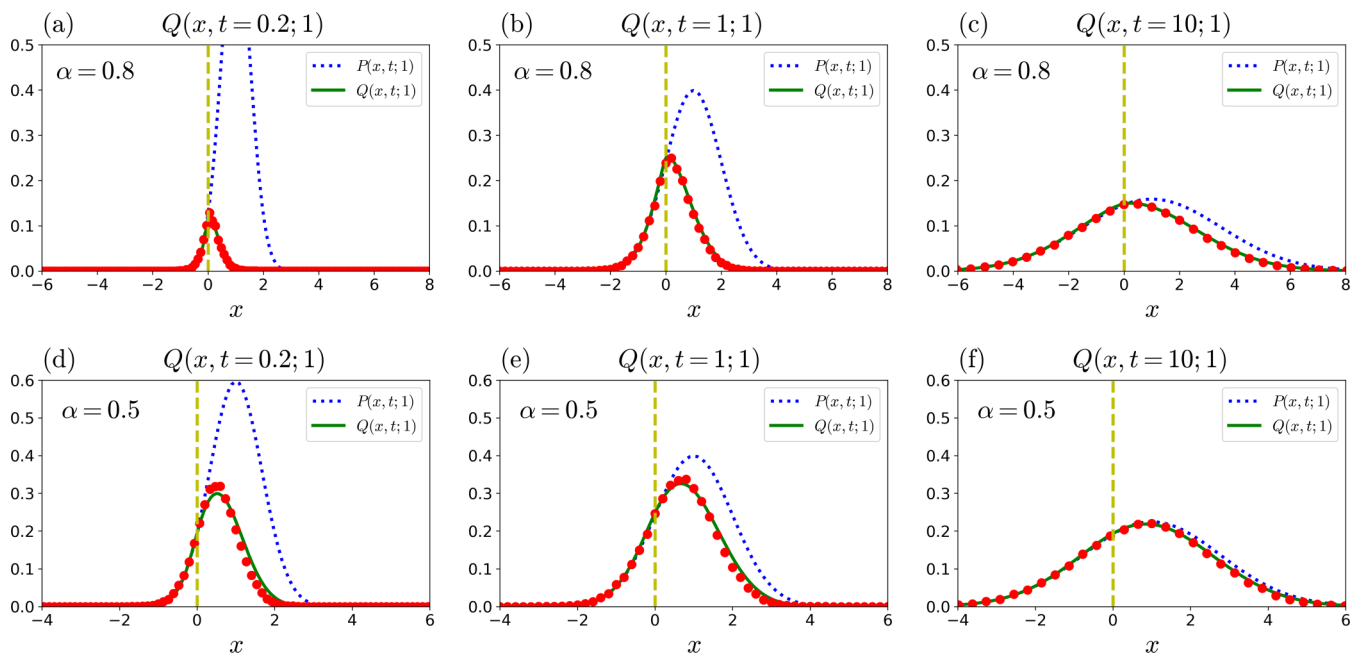


FIG. 4. Probability distribution $Q(x, t; 1)$ of the position of absorbed subdiffusive walkers. Plots of $Q(x, t; 1)$ for subdiffusive fBM (a)–(c) with $\alpha = 0.8$ and (d)–(f) with $\alpha = 0.5$ at early, middle, and late times ($t = 0.2, 1, 10$, respectively). Analytical prediction (green solid curve) is obtained using Eqs. (2), (3), and (12), which quantitatively reproduces the numerical simulation results (red circles). The error bar evaluated as 95% CI is smaller than the size of the symbol. Blue dashed curves represent the free space distribution $P(x, t; 1)$. The asymmetry in $Q(x, t; 1)$ grows with the memory effect, which is stronger for smaller $\alpha$.

**(a)** $\widetilde{P}_+(x,t;1)$

$\alpha = 0.8$

**(b)** $\widetilde{P}_+(x,t;1)$

$\alpha = 0.5$
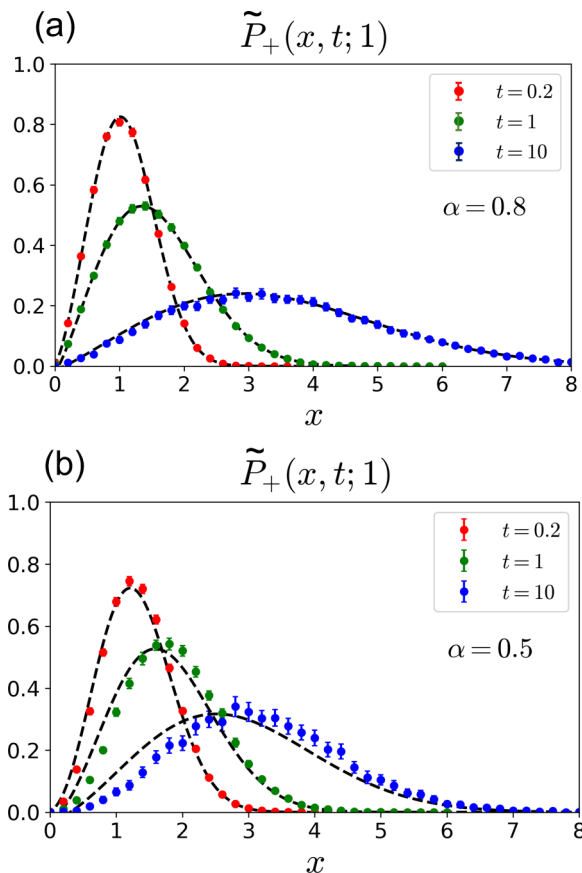
FIG. 5. Probability distribution $P_+(x,t;1)$ of the position of survived subdiffusive walkers. Plots of the normalized position probability $\tilde{P}_+(x,t;1) \equiv P_+(x,t;1)/S(t;1)$ for subdiffusive fBM with (a) $\alpha = 0.8$ and (b) $\alpha = 0.5$ at early, middle, and late times ($t = 0.2, 1, 10$, respectively). Analytical prediction (dashed curve) is obtained using Eq. (1), which captures the numerical simulation results (symbols). Error bars represent 95% CI.

One notable feature in $\tilde{P}_+(x,t;1)$ is that the slope $[\partial \tilde{P}_+(x,t;1)/\partial x]_{x\to 0}$ at the boundary is vanishingly small [34]. Such an anomalous behavior of $\tilde{P}_+(x,t;1) \sim x^\delta$ close to the boundary with nontrivial exponent $\delta$ can be quantified from our expression for $Q(x,t;1)$ as follows. Note first that in the long time limit $t \gg 1 (\Leftrightarrow x_0^2/D_\alpha t^\alpha \ll 1$ in original unit), the asymptotic behavior of $\tilde{P}_+(x,t;1)$ is obtained by taking $x_0 \to 0$ limit [30]. For the walker absorbed at time $\tau$, its characteristic travel distance during the subsequent time interval $s = t - \tau$ is evaluated as $\Delta x(s) \sim s^{\alpha/2}$. This indicates that, for a given location $x$, the walker only starts substantially contributing to $Q(x,t;1)$ after the time $t^{(x)} = x^{2/\alpha}$. From Eq. (2), we thus find

$$Q(x,t;1) \sim \int_{t^{(x)}}^{t-\tau^*} (t-s)^{-(2-\alpha/2)} s^{-\alpha/2} \, ds$$
$$\sim t^{-\alpha/2} \big(1 - t^{-(2-\alpha)} x^{(2-\alpha)/\alpha}\big). \quad (14)$$

The first term cancels the free space distribution $P(x,t;1) \sim t^{-\alpha/2}$, leaving $P_+(x,t;1) \sim t^{-(2-\alpha/2)} x^{(2-\alpha)/\alpha}$, or equivalently, $\tilde{P}_+(x,t;1) \sim t^{-1} x^{(2-\alpha)/\alpha}$. The predicted exponent $\delta = (2-\alpha)/\alpha$ agrees with that obtained from heuristic scaling argument [30].
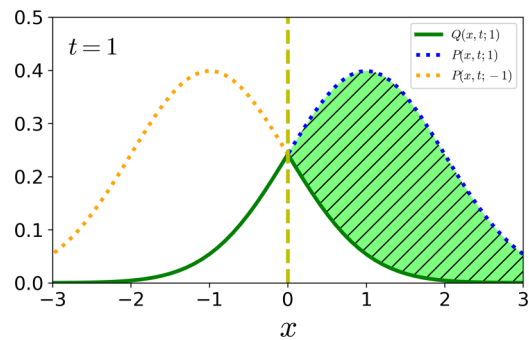


FIG. 6. Illustration of the method of image applicable to the Markovian case. Shown here is the position distribution $P(x,t;1)$ of the walker in free space (dotted green) and that $P(x,t;-1)$ of the *image walker*, whose initial position is $x = -1$ (dotted yellow). The latter and the former constitute the position distribution $Q(x,t;1)$ (solid green) of the *dead walker* for $x \geqslant 0$ and $x \leqslant 0$, respectively. The hatched area represents the survival probability $S(t;1) = \int_0^\infty P_+(x,t;1)dx$.

For the Markovian case $\alpha = 1$, the slope at the boundary is finite ($\delta = 1$), which multiplied by diffusion coefficient is the outgoing flux. The peculiar nature of the flux for the $\alpha \neq 1$ case implies the breakdown of Fick's law, and makes the implementation of a reflective boundary nontrivial. This rephrases a fact that there is no diffusion (more generally Fokker-Planck) equation for non-Markovian walkers in the ordinary sense.

### D. Failure of the method of image

To see the point, let us see that $Q(x,t;1)$ for Markovian walkers ($\alpha = 1$) can be constructed by the method of image, see Fig. 6, where $Q(x,t;1)$ in the physical domain ($x \geqslant 0$) is given by the position distribution of the image walkers $P(x,t;-1)$. $Q(x,t;1)$ in the negative domain ($x < 0$) is simply given by $Q(x,t;1) = P(x,t;1)$ due to the absorbing boundary at $x = 0$, hence $P_+(x,t;1) = 0$ for $x < 0$. From this construction, it is clear that the reversal symmetry $Q(x,t;1) = Q(-x,t;1)$ holds; see the green solid curve in Fig. 6. Integrating Eq. (1) over the entire space (including the negative domain), one finds $S(t;1) = 1 - \int_{-\infty}^\infty Q(x,t;1)dx$, where the surviving probability $S(t;1) = \int_0^\infty P_+(x,t;1)dx$ is denoted by the hatched area in Fig. 6. Equivalent to the above relation is $\int_0^\infty Q(x,t;1)dx = [1 - S(t;1)]/2$ thanks to the reversal symmetry of $Q(x,t;1)$ with respect to $x = 0$, producing a factor of 1/2. The same relation is obtained by integrating Eq. (2) over the positive $x$ domain with $\langle x(t)\rangle_{\mathrm{FPT}=\tau} = 0$. Therefore, the validity of the method of image relies on the condition $\langle x(t)\rangle_{\mathrm{FPT}=\tau} = 0$.

The effect of the (anti)persistent memory in fBM becomes stronger with the departure from the Markovian limit $\alpha = 1$. This is seen, for instance, in the spatial profile of $Q(x,t;1)$ shown in Fig. 4, where the degree of the asymmetry $Q(x,t;1) \neq Q(-x,t;1)$, a hallmark of the memory effect, becomes more evident for smaller $\alpha$. To examine the $\alpha$ dependence more closely, in Fig. 7, we show the position probability of the survival walkers $P_+(x,t=1;1)$ for $\alpha = 0.8, 0.6, 0.5,$ and $0.3$, where the comparison is made for
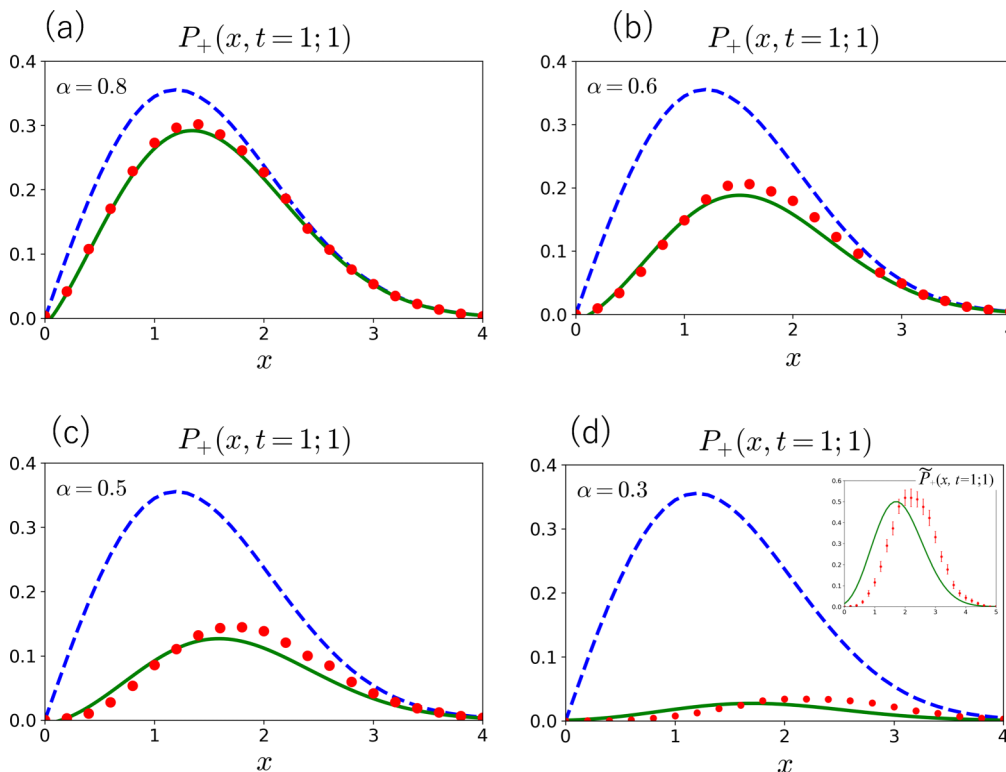
FIG. 7. Failure of the method of image. Plot of $P_+(x, t; 1)$ at $t = 1$ for (a) $\alpha = 0.8$, (b) $\alpha = 0.6$, (c) $\alpha = 0.5$, and (d) $\alpha = 0.3$. Solid curves (green) are obtained from our theory, which captures the numerical simulation result (red symbols) reasonably well. In contrast, the method of image yields qualitatively wrong profiles (blue dashed curves). Since, for the $\alpha = 0.3$ case, the survival probability $S(t; 1) = \int_0^\infty P_+(x, t; 1) dx$ is already rather low at this time ($t = 1$), we plot the normalized probability $\tilde{P}_+(x, t; 1) = P_+(x, t; 1)/Q(t; 1)$ [inset of (d)] for a clear visibility.

our solution and that constructed by the method of image. Clearly, the method of image fails to capture the profile even qualitatively. In contrast, our method is capable of more accurate description; the quantitative accuracy is very good for the case of $\alpha = 0.8$, and the relative accuracy over the method of image becomes increasingly manifest for smaller $\alpha$. Still, we need to note the quantitative discrepancy between theory and simulation data, which becomes more apparent for lower $\alpha$, and clearly visible in the plot of normalized probability $\tilde{P}_+(x, t; 1) = P_+(x, t; 1)/Q(t; 1)$ [inset of (d)]. This is most probably linked to deviation from our assumption $\langle x(t) \rangle_{\text{FPT}=\tau} = \langle x(t) \rangle_f$, with the latter being evaluated based on the mean-field approximation (10).

Finally, we note that if one employs a diffusion equation with the time-dependent diffusivity $D(t) \sim t^{\alpha-1}$, one obtains the position probability $P(x, t; 1) = \mathcal{N}(x, 1, t^\alpha)$ in a free space, which is the same as that of fBM. However, the process described by such a diffusion equation is very different from fBM, which is clearly seen in their first passage statistics. Indeed, writing a diffusion equation implies the adaptation of Markovian description, thus the applicability of the method of image, which however results in the wrong answer.

## IV. SUMMARY

In conclusion, we have provided a natural framework with which the first passage process of non-Markovian walkers can be analyzed, where a key quantity is the average behavior

$\langle x(t) \rangle_{\text{FPT}=\tau}$ of the system after the first passage. Although this quantity is difficult to calculate, the viscoelastic nature of the subdiffusive non-Markovian walker indicates that $\langle x(t) \rangle_{\text{FPT}=\tau}$ may be seen as a relaxation process from the first passage point as its initial condition. This observation led us to try representing $\langle x(t) \rangle_{\text{FPT}=\tau}$ using the dynamical response $\langle x(t) \rangle_f$ of the system. The latter can be calculated using the generalized Langevin equation with a caution that the result depends on the perturbation protocol to prepare the "nonequilibrium initial state" to analyze subsequent relaxation. We adopted the simplest constant force protocol, which in the temporal sense corresponds to the mean-field approximation. One may expect inevitable errors in such a mean-field approximation given the correlation effect, in the present context, arising from the fact that the future evolution of the non-Markovian system depends on how the current state is prepared; for fBM, the correlation time scale is divergent due to its power-law memory. We have indeed shown that the systematic error is visible in the average regression after the first passage, which becomes larger for smaller $\alpha$ (Appendix B). Fortunately, we have also found that such a flaw does not seem to affect key quantities in FPT statistics, such as $F(\tau; x_0)$, $Q(x, t; x_0)$ and $P_+(x, t; x_0)$, in a crucial way, but its trail can nevertheless be found in the plot of $P_+(x, t; x_0)$ for small $\alpha$ (Fig. 5). On the whole, it may be tempting to view the current situation analogous to the early-day research of phase transition and critical phenomena, where the establishment of mean-field theory laid the foundation for further research. We hope that the current study will play a similar role to pave a way forward.

## APPENDIX A: CALCULATION OF DYNAMICAL RESPONSE

Here, we sketch the calculation of the dynamical response $\langle x(t) \rangle_f$, which is used to obtain the approximate form of the memory function $h(t)$. The equation of motion for fBM is Eq. (7) with

$$\mu(t) = \frac{2}{\gamma} \delta(t) + \mu_M(t), \tag{A1}$$

where $\gamma$ is the bare friction coefficient and $\mu_M(t) \sim -t^{\alpha-2}$ (for $t \gg \tau_0$) represents the power-law memory. For the calculation below, we adopt the form

$$\mu_M(t) = \begin{cases} -c \dfrac{1}{\gamma \tau_0} \left( \dfrac{t}{\tau_0} \right)^{\alpha-2} & (t \geqslant t_{\min}), \\ 0 & (t < t_{\min}), \end{cases} \tag{A2}$$

where $\tau_0$ is the microscopic (shortest) time scale in the problem (for instance, the monomeric time scale in the case of tagged monomer dynamics), and we introduce a sharp cutoff at $t_{\min} \sim \tau_0$. The nature of this short time-scale cutoff and the precise value of the numerical coefficient $c$ (of order unity) is irrelevant to the subdiffusive dynamics $\mathrm{MSD}(t) \sim t^{\alpha}$ [hence does not appear in the final expression, see Eq. (10)] as long as the sum rule $\int_0^\infty \mu(t) dt = 0$ is satisfied. Note that this sum rule is a consequence of the relaxation nature of the subdiffusive fBM [17]. In our "mean-field" treatment, the perturbation protocol to obtain the dynamical response is

$$f(t) = \begin{cases} f_0 & (0 \leqslant t < \tau), \\ 0 & (\text{otherwise}). \end{cases} \tag{A3}$$

Applying the above perturbation protocol, the average velocity and position of the particle are calculated as

$$\langle \dot{x}(t) \rangle_f = \begin{cases} \dfrac{f_0 c}{\gamma(1-\alpha)} (t/\tau_0)^{-(1-\alpha)} \\ \qquad \cdots (t \leqslant \tau), \\ \dfrac{f_0 c}{\gamma(1-\alpha)} \{ (t/\tau_0)^{-(1-\alpha)} - [(t-\tau)/\tau_0]^{-(1-\alpha)} \} \\ \qquad \cdots (t > \tau), \end{cases}$$

$$\langle x(t) \rangle_f = \begin{cases} x_0 + \dfrac{f_0 c \tau_0}{\gamma \alpha (1-\alpha)} (t/\tau_0)^{\alpha} \\ \qquad \cdots (t \leqslant \tau), \\ \langle x(\tau) \rangle_f \\ + \dfrac{f_0 c \tau_0}{\gamma \alpha (1-\alpha)} \{ (t/\tau_0)^{\alpha} - (\tau/\tau_0)^{\alpha} - [(t-\tau)/\tau_0]^{\alpha} \} \\ \qquad \cdots (t > \tau). \end{cases}$$

The first passage condition $\langle x(\tau) \rangle_f = 0$ fixes the force magnitude $f_0 = -[\gamma x_0 \alpha (1-\alpha)/c\tau_0](\tau/\tau_0)^{-\alpha} = -(Tx_0/D_\alpha)\tau^{-\alpha}$ [see Eq. (9)] [35], hence the relaxation process Eq. (10) is obtained. Note that Eq. (10) suggests that it is a function of $t/\tau$ reflecting the power-law nature of the memory.

## APPENDIX B: COMPARISON: $\langle x(t) \rangle_{\mathrm{FPT}=\tau}$ AND $\langle x(t) \rangle_f$

The backbone assumption of our formalism is $\langle x(t) \rangle_{\mathrm{FPT}=\tau} = \langle x(t) \rangle_f$. In order to assess the validity of this assumption, we compare Eq. (10) with numerical simulation data. Figure 8 shows that while the formula (10) predicts the master curve for $\langle x(t) \rangle_f$ as a function of $t/\tau$, the actual numerical data for $\langle x(t) \rangle_{\mathrm{FPT}=\tau}$ reveals a clear $\tau$ dependence, and thus a deviation from the master curve, which is more apparent for small $\alpha$. This observation pinpoints the complexity involved in the behavior of fBM after the first passage, which is not captured by our dynamical response approach with the constant force protocol.

In fact, one expects that the relaxation behavior should depend on the process of how the (nonequilibrium) initial
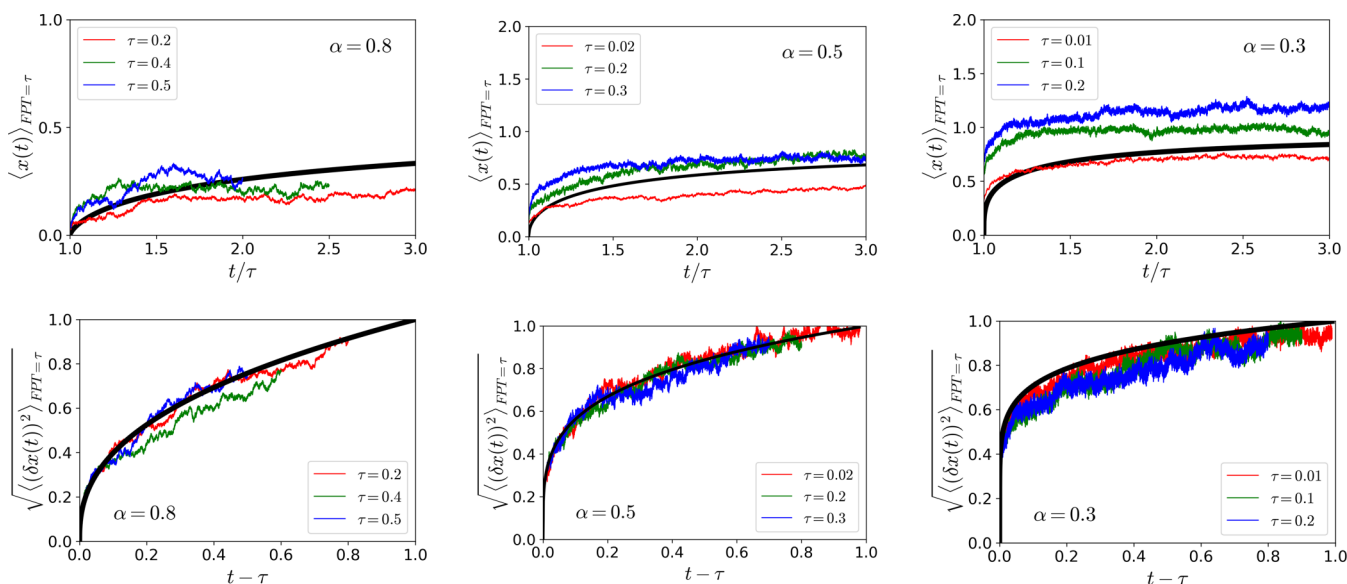


FIG. 8. Average (top) and variance (bottom) of fBM position after the first passage. Shown here are the case of $\alpha = 0.8$ (subensemble $\tau = 0.2, \ 0.4, \ 0.5$), $\alpha = 0.5$ (subensemble $\tau = 0.02, \ 0.2, \ 0.3$), and $\alpha = 0.3$ (subensemble $\tau = 0.01, \ 0.1, \ 0.2$), which are compared to analytical formulas (thick black curves) Eqs. (10) and (6), the former evaluated from the analysis of the dynamical response.
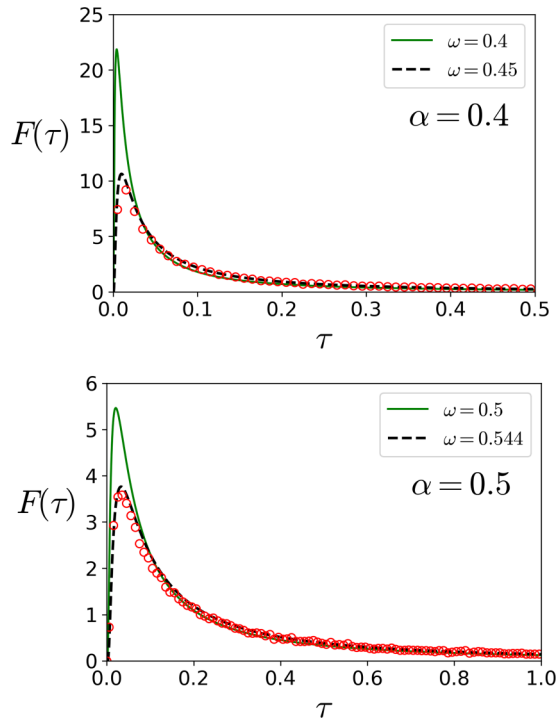
FIG. 9. Short time part of FPT distribution of non-Markovian walkers. Plot of $F(\tau)$ for (a) $\alpha = 0.4$ and (b) $\alpha = 0.5$. The best fit values are $\omega = 0.45$ for $\alpha = 0.4$ and $\omega = 0.544$ for $\alpha = 0.5$, which are included in the plot of Fig. 3(b).

condition is prepared, and thus the time dependence of the perturbation protocol. With such a caution in mind, it is not surprising to see the failure of formula (10) to quantitatively describe simulation results for the average position after the first passage. Nevertheless, it is remarkable that our mean-field approximation is capable of yielding excellent approximation for the FPT distribution $F(\tau)$ (Figs. 3 and 9). The same applies to the (normalized) position probability distribution $P_+(x, t; 1)$ (Figs. 5 and 7), although deviation starts to appear in the late time regime for small $\alpha$. We note that our mean-field theory yields the correct persistence exponent $p = 1 - \alpha/2$ as well as $\delta = (2 - \alpha)/\alpha$, which may be an underlying reason for the overall success. Still, one may expect inevitable errors in such a mean-field treatment given the correlation effect, which arises, in the present context, from the temporal memory effect in non-Markovian dynamics. A possibility for improvement over such a mean-field description remains to be known.

## APPENDIX C: ANALYSIS OF INTEGRAL EQUATION

Our assumption based on the dynamical response idea described above determines the memory function $h(t, \tau)$ [Eq. (11)] in the integral equation;

To analyze the integral equation (4), we first rewrite the memory function as

$$h(t, \tau) = \frac{t^{-\alpha/2}}{\sqrt{2}} g(u) \qquad (C1)$$

with

$$g(u) = (1 - u)^{-\alpha/2}(1 - u^{-\alpha}) + (1 - u)^{\alpha/2} u^{-\alpha}, \quad (C2)$$

where $u \equiv \tau/t$. The error function in the integrand is expanded as

$$\mathrm{erf}[h(t, \tau)] = \mathrm{erf}\left(\frac{t^{-\alpha/2}}{\sqrt{2}}\right) + \sqrt{\frac{2}{\pi}} t^{-\alpha/2}[g(u) - 1]$$

$$+ \mathcal{O}(t^{-3\alpha/2}). \qquad (C3)$$

Neglecting higher-order terms $\mathcal{O}(t^{-3\alpha/2})$, Eq. (4) becomes

$$S(t; 1)\left[1 - \mathrm{erf}\left(\frac{t^{-\alpha/2}}{\sqrt{2}}\right)\right]$$

$$\simeq \sqrt{\frac{2}{\pi}} t^{1-\alpha/2} \int_0^1 F[\tau(u); 1]\{1 - g(u)\} du. \qquad (C4)$$

Motivated by the known analytical solution

$$F(\tau; 1) = \mathcal{C}_1 \exp\left(-\frac{1}{2\tau}\right) \tau^{-3/2} \qquad (C5)$$

for the Markovian case ($\alpha = 1$), where $\mathcal{C}_1$ is a normalization constant, we seek for the solution in the form

$$F(\tau; 1) = \mathcal{C}_\alpha \exp\left(-\frac{1}{2\tau^\omega}\right) \tau^{-(1+p)}$$

$$= \mathcal{C}_\alpha t^{-(1+p)} \exp\left(-\frac{1}{2(tu)^\omega}\right) u^{-(1+p)}. \qquad (C6)$$

Substituting the above ansatz in Eq. (C4), we obtain

$$S(t; 1)\left[1 - \mathrm{erf}\left(\frac{t^{-\alpha/2}}{\sqrt{2}}\right)\right] \simeq \sqrt{\frac{2}{\pi}} \mathcal{C}_\alpha t^{-(p+\alpha/2)}$$

$$\times \int_0^1 e^{-\frac{1}{2(tu)^\omega}} \left\{\alpha u^{-(\alpha+p)}[1 + \mathcal{O}(u)]\right.$$

$$\left. - \frac{\alpha}{2} u^{-p}[1 + \mathcal{O}(u)]\right\} du \qquad (C7)$$

To evaluate the above integral, we note the following:

$$\int_0^1 e^{-\frac{1}{2(tu)^\omega}} u^{-\kappa} du \simeq \int_{u^*}^1 u^{-\kappa} du, \qquad (C8)$$

where $u^* = c_1 t^{-1}(\omega/2\kappa)^{1/\omega}$ with $c_1$ being a numerical constant of order unity. Then, at leading order in $1/t$, Eq. (C7) becomes

$$S(t; 1) \simeq \sqrt{\frac{2}{\pi}} \mathcal{C}_\alpha t^{-(1-\alpha/2)} \frac{\alpha}{\alpha + p - 1}$$

$$\times \left[c_1\left(\frac{\omega}{2(\alpha + p)}\right)^{1/\omega}\right]^{1-\alpha-p}, \qquad (C9)$$

which is asymptotically correct at large $t$. Calculating $-dS(t; 1)/dt$ and comparing it with the assumed form of $F(t; 1)$, we find the persistence exponent

$$p = 1 - \frac{\alpha}{2}, \qquad (C10)$$

in agreement with the earlier scaling argument [29]. In addition, by comparing two expressions of *prefactor*, we find a relation between $\omega$ and $\alpha$:

$$(2-\alpha)\left(\frac{2+\alpha}{\omega}\right)^{\alpha/(2\omega)} c_1^{-\alpha/2} = c_2, \qquad (C11)$$

where we introduce another numerical constant $c_2$ of order unity to make the evaluated relation equality. Since we know $\omega = 1$ for the Markovian limit $\alpha = 1$, one of the numerical constants can be eliminated through

$$c_2 = 3^{1/2} c_1^{-1/2}. \qquad (C12)$$

This leads to Eq. (13) with one fitting parameter $c_1$, which should be determined through the comparison with numerical simulation data. As discussed in the main text, we found $c_1 = 0.12$ describes the simulation results well. The resultant dependence of $\omega$ on $\alpha$ is shown in Fig. 3(b). Apparently, the relation is close to $\omega = \alpha$, but the value of $\omega$ is slightly larger than $\alpha$ in a systematic way. We note that, while irrelevant to the long time asymptotic power-law behavior, the short time behavior is highly sensitive to this $\omega$ exponent. For example, we show in Fig. 9 the short time part of the

FPT distribution $F(\tau)$ for the case of $\alpha = 0.4$ and 0.5, where our formula for $\omega(\alpha)$, but not $\omega = \alpha$, provides satisfactory fittings.

### APPENDIX D: NUMERICAL SIMULATION

To simulate fBM trajectories $\{x_0, x_1, \ldots, x_N\}$ of length $N$, we numerically integrated the discretized version of Eq. (1) in the main text with $f = 0$. The Gaussian variables $\eta_i$, called fractional Gaussian noise, have a temporal correlation, whose long time part is characterized by the power-law memory as described in Sec. II A. To generate the fractional Gaussian noise, we employed the Davies and Harte algorithm [36], and generated $m$ samples of length $N$ for each $\alpha$. From these simulations, we calculated the standard deviation of the walker's displacement $\Delta x_N \equiv \sqrt{\langle (x_N - x_0)^2 \rangle}$ after $N$ steps. To analyze the FPT statistics, we placed the hypothetical absorbing wall at $x = x_0 - \tilde{c}\,\Delta x_N$ such that the initial separation from the walker to the boundary is $\tilde{c}\,\Delta x$. We then reanalyzed each $m$ trajectory to find its first arrival at the wall, and constructed the FPT distribution and the walkers' distribution after the FPT. We adopted $N = 10^5$, $m = 10^5$, and $\tilde{c} = 1$ except for the FPT distribution data for the long time regime [Fig. 2(a) inset], where we adopted $N = 10^6$, $m = 10^4$, and $\tilde{c} = 0.5$.

---

[1] N.G. van Kampen, *Stochastic Processes in Physics and Chemistry* (North Holland, Amsterdam, 2007).

[2] S. Redner, *A Guide to First-Passage Processes* (Cambridge University Press, Cambridge, 2001).

[3] A. Szabo, K. Schulten, and Z. Schulten, First passage time approach to diffusion controlled reactions, J. Chem. Phys. **72**, 4350 (1980).

[4] H. A. Kramers, Brownian motion in a field of force and the diffusion model of chemical reactions, Physica **7**, 284 (1940).

[5] P. Hänggi, P. Talkner, and M. Borkovec, Reaction-rate theory: Fifty years after Kramers, Rev. Mod. Phys. **62**, 251 (1990).

[6] E. Carlon, H. Orland, T. Sakaue, and C. Vanderzande, Effect of memory and active forces on transition path time distributions, J. Phys. Chem. B **122**, 11186 (2018).

[7] L. Lavacchi, J. O. Daldrop, and R. R. Netz, Non-Arrhenius barrier crossing dynamics of non-equilibrium non-Markovian systems, Europhys. Lett. **139**, 51001 (2022).

[8] S. Condamin, O. Bénichou, V. Tejedor, R. Voituriez, and J. Klafter, First-passage times in complex scale-invariant media, Nature (London) **450**, 77 (2007).

[9] M. A. Lomholt, K. Tal, R. Metzler, and K. Joseph, Lévy strategies in intermittent search processes are advantageous, Proc. Natl. Acad. Sci. USA **105**, 11055 (2008).

[10] G. Wilemski and M. Fixman, Diffusion-controlled intrachain reactions of polymers. I theory, J. Chem. Phys. **60**, 866 (1974).

[11] M. Doi, Diffusion-controlled reaction of polymers, Chem. Phys. **9**, 455 (1975).

[12] I. M. Sokolov, Cyclization of a polymer: First-passage problem for a non-Markovian process, Phys. Rev. Lett. **90**, 080601 (2003).

[13] O. Bénichou, T. Guérin, and R. Voituriez, Mean first-passage times in confined media: From Markovian to non-Markovian processes, J. Phys. A: Math. Theor. **48**, 163001 (2015).

[14] S. D. Lawley, Extreme first-passage times for random walks on networks, Phys. Rev. E **102**, 062118 (2020).

[15] Q.-H. Wei, C. Bechinger, and P. Leiderer, Single-file diffusion of colloids in one-dimensional channels, Science **287**, 625 (2000).

[16] D. Panja, Anomalous polymer dynamics is non-Markovian: Memory effects and the generalized Langevin equation formulation, J. Stat. Mech. (2010) P06011.

[17] T. Saito and T. Sakaue, Driven anomalous diffusion: An example from polymer stretching, Phys. Rev. E **92**, 012601 (2015).

[18] F. Amblard, A. C. Maggs, B. Yurke, A. N. Pargellis, and S. Leibler, Subdiffusion and anomalous local viscoelasticity in actin networks, Phys. Rev. Lett. **77**, 4470 (1996).

[19] T. Turiv, I. Lazo, A. Brodin, B. I. Lev, V. Reiffenrath, V. G. Nazarenko, and O. D. Lavrentovich, Effect of collective molecular reorientations on Brownian motion of colloids in nematic liquid crystal, Science **342**, 1351 (2013).

[20] J.-H. Jeon, H. M.-S. Monne, M. Javanainen, and R. Metzler, Anomalous diffusion of phospholipids and cholesterols in a lipid bilayer and its origins, Phys. Rev. Lett. **109**, 188103 (2012).

[21] D. S. Banks and C. Fradin, Anomalous diffusion of proteins due to molecular crowding, Biophys. J. **89**, 2960 (2005).

[22] A. K. Yesbolatova, R. Arai, T. Sakaue, and A. Kimura, Formulation of chromatin mobility as a function of nuclear size during c. *elegans* embryogenesis using polymer physics theories, Phys. Rev. Lett. **128**, 178101 (2022).

[23] R. Benelli and M. Weiss, From sub- to superdiffusion: Fractional Brownian motion of membraneless organelles in early c. *elegans* embryos, New J. Phys. **23**, 063072 (2021).

[24] R. Metzler, J.-H. Jeon, A. G. Cherstvy, and E. Barkai, Anomalous diffusion models and their properties: Non-stationarity, non-ergodicity, and ageing at the centenary of single particle tracking, Phys. Chem. Chem. Phys. **16**, 24128 (2014).

[25] A. J. Bray, S. N. Majumdar, and G. Schehr, Persistence and first-passage properties in nonequilibrium systems, Adv. Phys. **62**, 225 (2013).

[26] A. P. Minton, The influence of macromolecular crowding and macromolecular confinement on biochemical reactions in physiological media, J. Biol. Chem. **276**, 10577 (2001).

[27] A. Amitai, Y. Kantor, and M. Kardar, First-passage distributions in a collective model of anomalous diffusion with tunable exponent, Phys. Rev. E **81**, 011107 (2010).

[28] T. Guérin, N. Levernier, O. Bénichou, and R. Voituriez, Mean first-passage times of non-Markovian random walkers in confinement, Nature (London) **534**, 356 (2016).

[29] J. Krug, H. Kallabis, S. N. Majumdar, S. J. Cornell, A. J. Bray, and C. Sire, Persistence exponents for fluctuating interfaces, Phys. Rev. E **56**, 2702 (1997).

[30] A. Zoia, A. Rosso, and S. N. Majumdar, Asymptotic behavior of self-affine processes in semi-infinite domains, Phys. Rev. Lett. **102**, 120602 (2009).

[31] K. J. Wiese, S. N. Majumdar, and A. Rosso, Perturbation theory for fractional Brownian motion in presence of absorbing boundaries, Phys. Rev. E **83**, 061141 (2011).

[32] S. Chandrasekhar, Stochastic problems in physics and astronomy, Rev. Mod. Phys. **15**, 1 (1943).

[33] B. B. Mandelbrot and J. W. van Ness, Fractional Brownian motions, fractional noises and applications, SIAM Rev. **10** 422 (1968).

[34] Y. Kantor and M. Kardar, Anomalous diffusion with absorbing boundary, Phys. Rev. E **76**, 061121 (2007).

[35] Using the adopted form for the memory kernel Eq. (A2), MSD is calculated as $\text{MSD} = 2D_\alpha t^\alpha$ with $D_\alpha = (cT/\gamma)[1/\alpha(1-\alpha)]\tau_0^{1-\alpha}$. Thus, we can write $f_0 = -Tx_0\tau^{-\alpha}/D_\alpha$, see Eq. (9) in the main text.

[36] R. B. Davies and D. S. Harte, Tests for Hurst effect, Biometrika **74**, 95 (1987).